arXiv:quant-ph/0104010v1 2 Apr 2001

Noise and Order in Cavity Quantum Electrodynamics

Per K. Rekdal[1] and Bo-Sture K. Skagerstam[2]

Department of Physics, The Norwegian University of Science and Technology, N-7491 Trondheim, Norway

Abstract

In this paper we investigate the various aspects of noise and order in the micromaser system. In particular, we study the effect of adding fluctuations to the atom cavity transit time or to the atom-photon frequency detuning. By including such noise-producing mechanisms we study the probability and the joint probability for excited atoms to leave the cavity. The influence of such fluctuations on the phase structure of the micromaser as well as on the long-time atom correlation length is also discussed. We also derive the asymptotic form of micromaser observables.

[1]Email address: perr@phys.ntnu.no.

[2]Email address: boskag@phys.ntnu.no.

1 Introduction

Noise is usually considered as a limiting factor in the performance of a physical device (see e.g. Refs.[1]). There are, however, nonlinear dynamical systems where the presence of noise sources can induce completely new regimes that cannot be realized without noise. Recent studies have shown that noise in such systems can induce more ordered regimes, more regular structures, increase the degree of coherence, cause the amplification of weak signals and growth of their signal-to-noise ratio (see e.g. Refs. [2, 3]). In other words, noise can play a constructive role, enhancing the degree of order in a system.

The micromaser is an example of such a nonlinear system. The micromaser system is an experimental realization of the idealized system of a two-level atom interacting with a second quantized single-mode of the electromagnetic field (for reviews and references see e.g. Refs. [4]- [7]). In the micromaser a beam of two-level atoms is sent through a microcavity where each atom intersects with the photon field inside the cavity during a transit time τ. After exit from the cavity the atoms are detected in either of its two states. It is assumed that subsequent atoms arrive at time intervals which are much longer then the atom-field interaction such that at most one atom at a time is inside the cavity, which is the operating condition for the one-atom maser. In such a system noise-controlled jumps between metastable states have been discussed in the literature [3].

In the present paper we study the effect of including noise-producing mechanisms in the micromaser system like a velocity spread in the atomic beam or a spread in the atom-photon frequency detuning $\Delta\omega$. We show that under suitable conditions, such noise-producing mechanisms lead to more pronounced revivals in the probabilities $\mathcal{P}(+)$ and $\mathcal{P}(+,+)$, where $\mathcal{P}(+)$ is the probability that an atom is found in its excited state after interaction with the photon field inside the microcavity and $\mathcal{P}(+,+)$ is the joint probability that two consecutive atoms are measured in their excited state after interaction. It is the purpose of the present paper to study the counterintuitive role that noise can play in the micromaser and extend the results in Refs. [8, 9].

The paper is organized as follows. For the convenience of the reader we recapitulate in Section 2 the theoretical framework of the micromaser system. In this Section we also discuss the general conditions to make revivals in the probability $\mathcal{P}(+)$ well separated in the atomic transit time. In Section 3 we determine asymptotic limits of the order parameter of the micromaser system and the probabilities $\mathcal{P}(+)$ and $\mathcal{P}(+,+)$. In Section 4 the effect of noise on $\mathcal{P}(+)$ and $\mathcal{P}(+,+)$, the order parameter and the micromaser phase

diagram is discussed. In Section 5 the effect of fluctuations on the correlation length is discussed and numerical investigations are presented. A conclusion is given in Section 6.

2 The Dynamical System

In the description of the dynamics of the one-atom micromaser we have to take losses of the photon field into account, i.e. the time evolution of the photon field is described by a master equation. The continuous time formulation of the micromaser system [10] is a suitable technical frame work for our purposes. Let a be the probability for a pump atom to be in its excited state. Assuming that the pump atoms are prepared in an incoherent mixture, i.e. the density matrix of the atoms is diagonal with diagonal matrix elements a and b such that $a + b = 1$, it is shown in [10, 9] that the vector p formed by the diagonal density matrix elements of the photon field obeys the differential equation $dp/dt = -\gamma Lp$. Here γ is the damping rate of photons in the cavity and $L = L_C - N(M-1)$, where $(L_C)_{nm} = (n_b+1)[\, n\delta_{n,m} - (n+1)\delta_{n+1,m}\,] + n_b[\,(n+1)\delta_{n,m} - n\delta_{n,m+1}\,]$ describes the damping of the cavity. n_b is the number of thermal photons and N is the average number of atoms injected into the cavity during the cavity decay time. The matrix M is $M = M(+) + M(-)$, where $M(+)_{nm} = bq_{n+1}\delta_{n+1,m} + a(1-q_{n+1})\delta_{n,m}$ and $M(-)_{nm} = aq_n\delta_{n,m+1} + b(1-q_n)\delta_{n,m}$, has its origin in the Jaynes-Cummings (JC) model [11, 9]. The quantity $q_n \equiv q(x = n/N)$ is given by

$$q(x) = \frac{x}{x+\Delta^2}\sin^2\left(\theta\sqrt{x+\Delta^2}\right) \quad , \tag{1}$$

where $\Delta^2 \equiv (\Delta\omega)^2/(4g^2N)$ is the scaled dimensionless detuning parameters of the micromaser and g is the single photon Rabi frequency at zero detuning of the JC model. Eq. (1) is expressed in terms of the scaled dimensionless pump parameter $\theta = g\tau\sqrt{N}$. Noise mechanisms, like a spread in the transition time or a spread in the detuning, are now included in the analysis by simply averaging the matrix L with respect to θ or Δ, i.e. averaging the quantity q_n with respect to one of these parameters. A similar averaging procedure with regard to the parameters a (or b) or n_b leads only to a trivial replacement of the corresponding parameters with their mean values. The stationary solution of the photon distribution where such noise effects are included is therefore derived in a standard and well known manner [8, 10, 9]. The result is

$$\bar{p}_n = \bar{p}_0 \prod_{m=1}^{n} \frac{n_b\, m + Na\langle q_m\rangle}{(1+n_b)\, m + Nb\langle q_m\rangle} \quad , \tag{2}$$

where $\langle\cdot\rangle$ in Eq. (2) denotes averaging, to be discussed below, with respect to θ or Δ. $\bar{p}_0$ is a normalization constant.

After the passage through the microcavity we make a selective measurement of the atoms. We imagine that one then only measure those atoms leaving the cavity with a definite value of θ or Δ, i.e. in effect putting a sharp velocity filter or a filter sensitive to detuning at the atom output port of the cavity. The probability $\mathcal{P}(s)$ of finding an atom in a state $s = \pm$ after the interaction with the cavity photons, where $+$ represents the excited atom state and $-$ represents the atom ground state, can then be expressed in the following matrix form [9]:

$$\mathcal{P}(s) = \bar{u}^T M(s) \bar{p} \quad , \tag{3}$$

such that $\mathcal{P}(+) + \mathcal{P}(-) = 1$. The elements of the vector $\bar{p}$ is given by the equilibrium distribution in Eq. (2). The quantity $\bar{u}$ is a vector with all entries equal to 1, $\bar{u}_n = 1$. Explicitly $\mathcal{P}(+)$ takes the form

$$\mathcal{P}(+) = a \sum_{n=0}^{\infty} \bar{p}_n (1 - q_{n+1}) + b \sum_{n=0}^{\infty} \bar{p}_{n+1} q_{n+1} \quad . \tag{4}$$

It is well known in the literature that this probability can exhibit quantum revivals (see e.g. Refs. [4] - [6]). Furthermore, the joint probability for observing two consecutive atoms in the states s_1 and s_2 is given by [9]

$$\begin{aligned} \mathcal{P}(s_1, s_2) &= \bar{u}^T S(s_2)\, S(s_1)\, \bar{p} \\ &= \bar{u}^T M(s_2)\, S(s_1)\, \bar{p} \quad , \end{aligned} \tag{5}$$

where $S(s) = (1 + L_C/N)^{-1} M(s)$. Explicitly one finds

$$\begin{aligned} \mathcal{P}(+,+) &= a^2 \sum_{n,m=0}^{\infty} (1 - q_{n+1})\, (1 + L_C/N)^{-1}_{nm}\, (1 - q_{m+1})\, \bar{p}_m \\ &+ ab \sum_{n,m=0}^{\infty} \Big\{ (1 - q_{n+1})\, (1 + L_C/N)^{-1}_{nm}\, q_{m+1}\, \bar{p}_{m+1} \end{aligned}$$

$$+ \quad q_n \, (1 + L_C/N)^{-1}_{nm} \, (1 - q_{m+1}) \, \bar{p}_m \Big\}$$

$$+ \quad b^2 \sum_{n,m=0}^{\infty} q_n \, (1 + L_C/N)^{-1}_{nm} \, q_{m+1} \, \bar{p}_{m+1} \quad . \tag{6}$$

In Refs.[9, 12] it is shown that the equilibrium distribution Eq. (2) can be re-written in a form which is rapidly convergent in the large N limit by making use of a Poisson summation technique [13]. In terms of the scaled photon number variable $x = n/N$ the stationary probability distribution can be written in the from

$$\bar{p}(x) = \bar{p}_0 \sqrt{\frac{w(x)}{w(0)}} \; e^{-N\,V(x)} \quad , \tag{7}$$

where

$$V(x) = \sum_{k=-\infty}^{\infty} V_k(x) \quad . \tag{8}$$

The effective potential $V(x)$ is expressed in terms of

$$V_k(x) = -\int_0^x d\nu \; \ln[\, w(\nu)\,] \, \cos(2\pi N k \nu) \quad , \tag{9}$$

where

$$w(x) = \frac{n_b \, x + a \, \langle q(x) \rangle}{(1 + n_b) \, x + b \, \langle q(x) \rangle} \quad . \tag{10}$$

We stress that Eq. (7) is exact. In the large N limit Eq. (7) can be simplified by making use of a saddle-point approximation. Apart from calculable $1/N$ corrections we put $V(x) = V_0(x)$. The saddle-points are then determined by $V_0'(x) = 0$, where $V_0'(x)$ is the derivative of $V_0(x)$ with respect to x. Hence, it is the nature of the global minima of $V_0(x)$ which determine the probability distribution, apart from possible zeros of $w(x)$.

If the only global minimum of $V_0(x)$ occurs at $x = 0$, which corresponds to the thermal phase of the micromaser, we can expand the effective potential $V_0(x)$ around origin. The probability $\bar{p}_n$ is then given by

$$\bar{p}_n = \bar{p}_0 \left(\frac{n_b + a \, \theta^2_{eff}}{1 + n_b + b \, \theta^2_{eff}} \right)^n \quad , \tag{11}$$

where

$$\theta_{eff}^2 = \lim_{x\to 0} \frac{\langle q(x)\rangle}{x} = \left\langle \frac{\sin^2(\theta\Delta)}{\Delta^2} \right\rangle \quad . \tag{12}$$

The probability distribution as given by Eq. (11) is normalizable provided

$$\theta_{eff}^2(2a-1) < 1 \quad . \tag{13}$$

If, on the other hand, there exists non-trivial saddle-points of $V_0(x)$, which correspond to the possible maser phases of the micromaser, we write

$$\bar{p}(x) = \sum_j \bar{p}_j(x) \quad , \tag{14}$$

where $\sum_j$ denotes the sum over the local minima of $V_0(x)$, i.e. $V_0''(x) > 0$, and where $\bar{p}_j(x)$ is $\bar{p}(x)$ for x close to the local minimum $x = x_j$. The distribution $\bar{p}_j(x)$ is given by

$$\bar{p}_j(x) = \frac{T_j}{\sqrt{2\pi N}}\, e^{-\frac{N}{2}V_0''(x_j)(x-x_j)^2} \quad , \tag{15}$$

where T_j is determined by the normalization condition for $\bar{p}(x)$, i.e

$$T_j = \frac{e^{-NV_0(x_j)}}{\sum_m e^{-NV_0(x_m)}/\sqrt{V_0''(x_m)}} \quad , \tag{16}$$

and

$$V_0''(x) = \frac{(2a-1)^2}{a + n_b(2a-1)}\, \frac{\langle q(x)\rangle - x\, d\langle q(x)\rangle/dx}{x^2} \quad . \tag{17}$$

For the given parameters, the sum in Eq. (16) is supposed to be taken over all saddle-points corresponding to a minimum of $V_0(x)$, i.e. all saddle-points corresponding to $V_0''(x) > 0$. If $x = x_j$ does not correspond to a global minimum of the effective potential $V_0(x)$, then T_j is exponentially small in the large N limit. If $x = x_j$ does correspond to one and only one global minimum, we can neglect all the terms in the sum in T_j but $m = j$, in which case T_j is reduced to $T_j = \sqrt{V_0''(x_j)}$. In the neighbourhood of such a global minimum the probability distribution in Eq. (15) is therefore reduced to

$$\bar{p}_j(x) = \frac{1}{\sqrt{2\pi N^2\sigma_x^2}}\, e^{-\frac{(x-x_j)^2}{2\sigma_x^2}} \quad , \tag{18}$$

where the standard deviation σ_x of Eq. (18) is

$$\sigma_x = \frac{1}{\sqrt{N V_0''(x_j)}} \quad , \tag{19}$$

which is zero in the large N limit provided $V_0''(x_j) \neq 0$. The probability $\bar{p}(x)$ is therefore peaked around the global minima for large N. The minimum x_j of the potential $V_0(x)$ is a solution of saddle-point equation

$$x = (2a-1)\langle q(x)\rangle \leq 1 \quad . \tag{20}$$

This saddle-point equation is independent of the number n_b of thermal photons in the cavity.

The excitation probability $\mathcal{P}(+)$ can be re-written in a form where quantum revivals (see e.g. Ref. [5]) become explicitly by making use of a Poisson summation technique [13]. When $a = 1$ we obtain

$$\begin{aligned} \mathcal{P}(+) &= 1 - \frac{1}{2}\sum_{n=0}^{\infty} \bar{p}_n \frac{n+1}{n+1+N\Delta^2} + \frac{1}{2}\sum_{\nu=-\infty}^{\infty} w_\nu(\theta) \\ &+ \frac{1}{2}\,\bar{p}_0\,\frac{1}{1+N\Delta^2}\cos(\,2\theta\sqrt{1/N+\Delta^2}\,) \quad , \end{aligned} \tag{21}$$

where

$$w_0(\theta) = N\int_0^{\infty} dx\; \bar{p}(x)\frac{x+1/N}{x+1/N+\Delta^2}\cos\left(2\theta\sqrt{x+1/N+\Delta^2}\right) \quad , \tag{22}$$

and

$$\begin{aligned} w_\nu(\theta) &= N\,\mathrm{Re}\Big\{\, e^{-2\pi i\nu N\left[\,(\theta/2\pi\nu N)^2+\Delta^2\,\right]} \\ &\times \int_0^{\infty} dx\; \bar{p}(x)\,\frac{x+1/N}{x+1/N+\Delta^2}\; e^{2\pi i\nu N\left(\,\sqrt{x+1/N+\Delta^2}-\theta/2\pi\nu N\,\right)^2} \Big\} \quad . \end{aligned} \tag{23}$$

Here $\bar{p}(x)$ is the continuous version of $\bar{p}(n/N)$. We stress that Eq. (21) is exact. If $a \neq 1$ we obtain $\mathcal{P}(+)$ by the replacement $\mathcal{P}(+) \to 1 - a + (2a-1)\mathcal{P}(+)$, apart from $1/N$ corrections. If the probability distribution $\bar{p}(x)$ is sufficiently peaked, i.e. $\bar{x} \gg \sigma_x$, where $\bar{x} \equiv \bar{x}(\theta)$ denotes the average of $x = n/N$ with respect to the stationary probability distribution $\bar{p}_n$, then the excitation probability is reduced to

$$\mathcal{P}(+) \approx 1 - \frac{1}{2}\frac{\bar{x}}{\bar{x}+\Delta^2} + \frac{1}{2}\sum_{\nu=0}^{\infty} w_\nu(\theta) \quad , \tag{24}$$

where

$$\begin{aligned} w_\nu(\theta) &\approx \bar{p}(x=\bar{x}_\nu)\,\frac{\bar{x}}{\bar{x}+\Delta^2}\,\frac{\theta}{\pi\sqrt{2\nu^3 N}} \\ &\times \cos\left[2\pi\nu N\left(\left(\frac{\theta}{2\pi\nu N}\right)^2+\Delta^2\right)-\frac{\pi}{4}\right] \quad , \quad \nu \geq 1 \quad , \end{aligned} \tag{25}$$

and

$$\bar{x}_\nu = \left(\frac{\theta}{2\pi\nu N}\right)^2 - \Delta^2 \quad . \tag{26}$$

According to Eq. (26) the ν:th revival of $\mathcal{P}(+)$ occurs in the region where θ is close to

$$\theta_\nu = 2\pi\nu N\sqrt{\bar{x}+\Delta^2} \quad . \tag{27}$$

This equation relates the width σ_x of the probability distribution $\bar{p}(x)$ into a measure for the width $\Delta\theta_\nu$ in the pump parameter of the ν:th revival according to a probability distribution of the form $p(\theta) \simeq \exp(-(\theta-\theta_\nu)^2/2(\Delta\theta_\nu)^2)$, i.e.

$$\Delta\theta_\nu = \pi\nu N\,\frac{\sigma_x}{\sqrt{\bar{x}+\Delta^2}} \quad . \tag{28}$$

Two consecutive terms of the sum in Eq. (24) separate in time when their temporal separation $\theta_{\nu+1}-\theta_\nu$ is larger then $\Delta\theta_{\nu+1}+\Delta\theta_\nu$, i.e. within one standard deviation, provided

$$\nu < \frac{\bar{x}+\Delta^2}{\sigma_x} - \frac{1}{2} \quad . \tag{29}$$

The revivals in $\mathcal{P}(+)$ cannot be resolved for values of ν larger then the right-hand side of Eq. (29).

If the probability distribution $\bar{p}(x)$ is sufficiently peaked, i.e. $\bar{x} \gg \sigma_x$, then the excitation probability $\mathcal{P}(+)$ approaches

$$\mathcal{P}(+) = a - \frac{1}{2}(2a-1)\left(\frac{\bar{x}}{(\bar{x}+\Delta^2)} - w_0(\theta)\right) \approx a - (2a-1)q(x) \quad , \tag{30}$$

in the large N limit, where we make use of

$$w_0(\theta) \approx \exp(-\theta^2/2N)\frac{\bar{x}}{\bar{x}+\Delta^2}\cos(2\theta\sqrt{\bar{x}+\Delta^2}) \quad . \tag{31}$$

If the average in the saddle-point equation Eq. (20) is such that $\langle q(x)\rangle \approx q(x)$, we see that $\mathcal{P}(+) \approx a - \bar{x}$. If we average Eq. (31) with respect to the noise in the system, we obtain $\langle \mathcal{P}(+)\rangle \approx a - \bar{x}$ by making use of the saddle-point equation Eq. (20) once more.

The approximative result Eq. (30) can actually be converted into an exact and more general relation between $\bar{x}$ and $\mathcal{P}(+)$. If the atoms are not measured with well-defined θ or Δ then we must in general average $\mathcal{P}(+)$ with respect to the corresponding probability distribution. In Eq. (4) we then replace q_n by $\langle q_n\rangle$ and denotes the corresponding excitation probability $\mathcal{P}(+)$ by $\langle \mathcal{P}(+)\rangle$. From the equilibrium distribution Eq. (2) we then obtain the recurrence formula $[\,(1+n_b)\,n + Nb\langle q_n\rangle\,]\,\bar{p}_n = \bar{p}_{n-1}[\,n_b\,n + Na\langle q_n\rangle\,]$. By summing this formula over n, we therefore derive that

$$\bar{x} = a + \frac{n_b}{N} - \langle \mathcal{P}(+)\rangle \quad . \tag{32}$$

In general and in the presence of noise in θ and/or Δ, $\bar{x}$ and $\mathcal{P}(+)$ have no direct relation and we must in general consider them to be independent variables.

3 Absence of Fluctuations

If the atoms enter the cavity without a spread in the transit time and without a spread in the atom-photon frequency detuning, the behavior of the order parameter and the excitation probability $\mathcal{P}(+)$ is well known in the literature (see e.g. Refs. [4, 6, 8]). As e.g. seen in Fig. 1, $\mathcal{P}(+)$ under such circumstances shows no clear evidence for resonant behavior of revivals. A more precise way to express the presence of revivals in the temporal variations of $\mathcal{P}(+)$ can e.g. obtained by performing a Fourier transformation of $\mathcal{P}(+)$ and considering the width of the corresponding spectrum. The corresponding Fourier spectrum of Fig. 1 is then broad. The appearance of clear revivals would correspond to a more peaked Fourier spectrum.

In the large N and θ limit the order parameter approaches a constant. This constant, $\bar{x}_\infty$, is therefore determined by the global minimum of $V_0(x)$ in the large θ limit, in which case $V_0(x)$ has a unique minimum. The micromaser system has then no maser-maser phase

transitions. As shown in an Appendix, this minimum is determined by $\partial V_0(x)/\partial x = 0$, where

$$\frac{\partial V_0(x)}{\partial x} = \ln\left[\frac{1-a}{a}\right] + f(\,y(x)\,) - f(\,w(x)\,) \quad , \tag{33}$$

and where $f(z)$, $y(x)$ and $w(x)$ are as given in the Appendix. When e.g. $a = 1$, $n_b = 0.15$ and $\Delta = 0$ the global minimum of $V_0(x)$ occurs at $\bar{x}_\infty \approx 0.34$, which corresponds to an asymptotic excitation probability $\mathcal{P}_\infty(+) \approx 0.66$ due to Eq. (32). When $a = 1$ and $\Delta = 0$ it follows from Eq. (6) that for large θ the joint probability $\mathcal{P}(+,+)$ approaches the asymptotic value

$$\mathcal{P}_\infty(+,+) \approx (5\mathcal{P}_\infty(+) - 1)/4 \quad , \tag{34}$$

i.e. with the physical parameters as above we find $\mathcal{P}_\infty(+,+) \approx 0.57$ (see Fig. 1). Eq. (34) follows from Eq. (6) by making use of the following properties of the unbounded operator L_C

$$\sum_{n=0}^{\infty} (L_C)_{nm} = 0 \quad , \quad \sum_{m=0}^{\infty} (L_C)_{nm} = -1 \quad , \tag{35}$$

and performing a suitable large N limit.

4 Effects of Fluctuations

We will now consider physical effects of noise in the micromaser system. We start by discussing the effects of adding fluctuations to the pump parameter θ and then, in Section 4.2, we study the effects of adding fluctuations to the atom-photon detuning parameter Δ.

4.1 Pump Parameter Fluctuations

Suppose that the pump parameter θ is described by a positive stochastic variable ξ as described by the probability distribution $P_\theta(\xi)$ such that $\langle\xi\rangle = \theta$ and $\langle(\xi-\theta)^2\rangle = \sigma_\theta^2$. The averaged value of $q(x)$ with respect to $P_\theta(\xi)$ is then given by

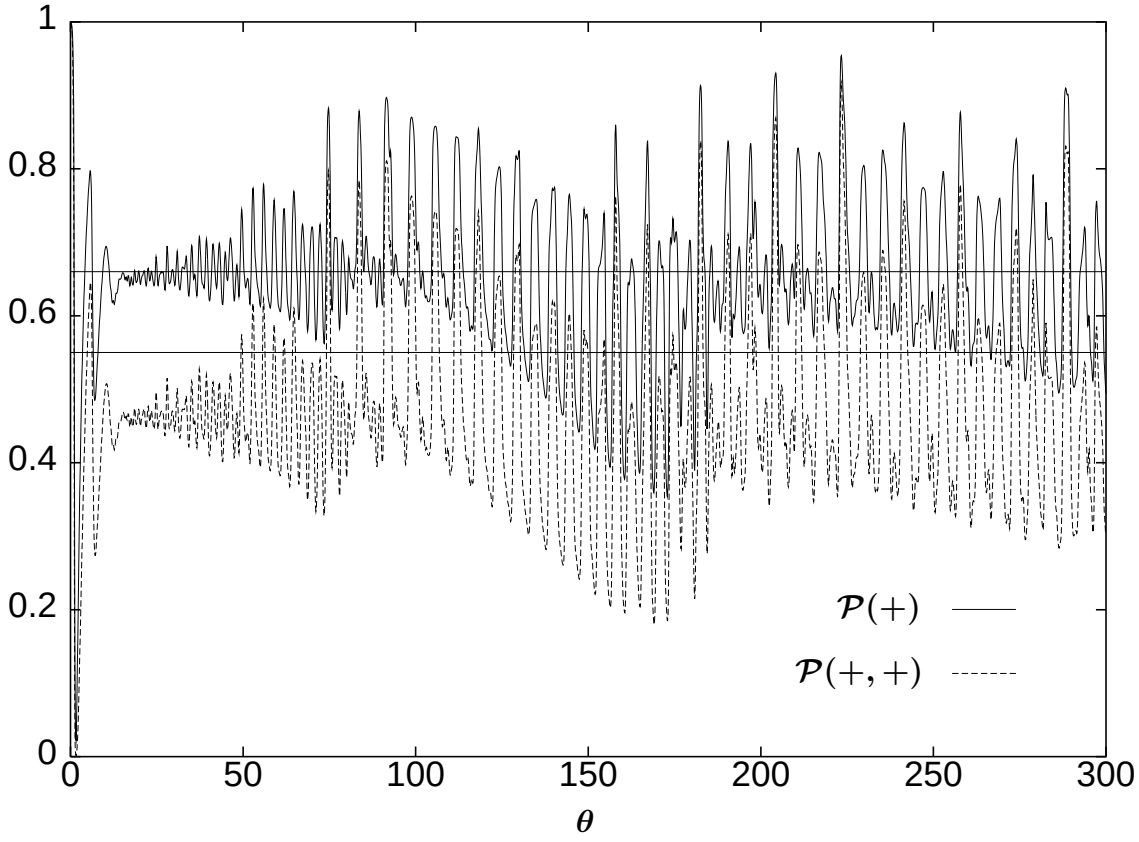

Figure 1: The probabilities $\mathcal{P}(+)$ (solid line) and $\mathcal{P}(+,+)$ (dotted line) as a function of θ when the q_m-terms in Eq. (2) are not averaged. The parameters are: $a = 1$, $\Delta = 0$, $n_b = 0.15$ and $N = 35$. The curves show no clear evidence for the resonant behavior of revivals. In the large θ and N limit the probability $\mathcal{P}(+)$ approaches $\mathcal{P}_\infty(+) \approx 0.66$ and the probability $\mathcal{P}(+,+)$ approaches $\mathcal{P}_\infty(+,+) \approx 0.57$, which are indicated by solid lines in the figure.

$$\langle q(x)\rangle_\theta = \int_0^\infty d\xi \; P_\theta(\xi)\, \frac{x}{x+\Delta^2} \sin^2\left(\xi\sqrt{x+\Delta^2}\right) \quad . \tag{36}$$

Non-trivial saddle-points of the corresponding $V_0(x)$ can be found by solving the equation

$$1 = (2a-1)\, I_1(\theta, x(\theta)) \quad , \tag{37}$$

where

$$I_1(\theta, x) = \frac{1}{x+\Delta^2} \int_0^\infty d\xi \; P_\theta(\xi) \; \sin^2\left(\xi\sqrt{x+\Delta^2}\,\right) \leq \sigma_\theta^2 + \theta^2 \quad . \tag{38}$$

For small values of x, we can expand the effective potential $V_0(x)$ around $x = 0$. A straightforward expansion $V_0(x)$ then leads to

$$V_0(x) = x \ln \left[\frac{1 + n_b + a\,\theta_{eff}^2}{n_b + a\,\theta_{eff}^2} \right] + \frac{x^2}{2} \frac{a + n_b(2a-1)}{(n_b + a\theta_{eff}^2)(1 + n_b + b\theta_{eff}^2)} \langle\, \xi^4 f(\xi|\Delta|) \,\rangle + \mathcal{O}(x^3) \quad , \tag{39}$$

where

$$f(x) = \frac{\sin^2(x)}{x^4} - \frac{\sin(x)\cos(x)}{x^3} \quad . \tag{40}$$

For small x, i.e. $x \ll 1$, $f(x) = 1/3 + \mathcal{O}(x^2)$. For typical physical parameters such that $\theta|\Delta| \lesssim \pi$, we therefore observe a thermal-maser phase transition for values of θ determined by $V_0'(x) = 0$. The corresponding critical transition line is then

$$a(\theta) = \frac{1}{2} + \frac{1}{2} \frac{1}{I_1(\theta)} \leq 1 \quad , \tag{41}$$

where $I_1(\theta, 0) \equiv I_1(\theta)$. Eq. (41) coincides with the radius of convergence of the thermal probability distribution Eq. (11) as it should. For $\Delta = 0$ we see that $\theta_{eff}^2 = \sigma_\theta^2 + \theta^2$ and hence this phase transition can occur for $\theta = 0$, i.e. the phase transition can be induced by the presence of noise in the stochastic variable θ. For $\theta|\Delta| \gg \pi$ we must in general make use of a combination of analytical and numerical methods, as in the case of $\sigma_\theta = 0$ [12], in order to get a detailed picture of the phase diagram.

In the maser phase, the order parameter $\bar{x}(\theta)$ approaches zero when the system approaches the critical line Eq. (41). Furthermore, in the large N limit $\bar{x}(\theta)$ is always zero in the thermal phase. Hence, the order parameter is continues on the critical transition line Eq. (41). To determine the order of the phase transition we therefore have to investigate higher order derivatives. The first derivative of $\bar{x}(\theta)$ with respect to θ, $\bar{x}'(\theta)$, at the critical transition line Eq. (41) is

$$\bar{x}'(\theta) = \frac{\Delta^2\, I_1'(\theta)}{I_1(\theta) - I_2(\theta)} \quad , \tag{42}$$

where $I_1'(\theta)$ is the derivative of $I_1(\theta)$ with respect to θ and where

$$I_2(\theta) = \int_0^\infty d\xi\; P_\theta(\xi)\, \xi^2\, \frac{\sin(2\xi\Delta)}{2\xi\Delta} \quad . \tag{43}$$

By making use of the positive definiteness of $P_\theta(\xi)\xi^2$, the Cauchy-Schwarz inequality implies $|I_2(\theta)| \leq \sqrt{\sigma_\theta^2 + \theta^2}$. If $x'(\theta)$ is zero, then we have to investigate higher order

derivatives. The second derivative of $\bar{x}(\theta)$ with respect to θ, $\bar{x}''(\theta)$, at the critical thermal-maser line Eq. (41) is

$$\bar{x}''(\theta) = \frac{\Delta^2 I_1''(\theta) + \bar{x}'(\theta) I_2'(\theta)}{I_1(\theta) - I_2(\theta)} \quad , \tag{44}$$

where $I_1''(\theta)$ is the second derivative of $I_1(\theta)$ with respect to θ and $I_2'(\theta)$ is the derivative of $I_2(\theta)$ with respect to θ.

The effective potential $V_0(x)$ approaches its large θ limit exponentially fast as a function of σ_θ^2. This unique minimum is determined by $\partial V_0(x)/\partial x = 0$, where $\partial V_0(x)/\partial x$ is given by Eq. (33) with $y(x)$ and $w(x)$ replaced by $\tilde{y}(x) = a\, e^{-2(x+\Delta^2)\sigma_\theta^2}/[\,\frac{a}{2}(1+e^{-2(x+\Delta^2)\sigma_\theta^2}) + n_b(x+\Delta^2)\,]$ and $\tilde{w}(x) = b\, e^{-2(x+\Delta^2)\sigma_\theta^2}/[\,\frac{b}{2}(1+e^{-2(x+\Delta^2)\sigma_\theta^2}) + (1+n_b)(x+\Delta^2)\,]$, respectively.

If the micromaser is not detuned, i.e. $\Delta = 0$, then there is one critical thermal-maser transition line only. This critical transition line can be found analytically for any probability distribution $P_\theta(\xi)$. The integral $I_1(\theta)$ is then given by

$$I_1(\theta) = \sigma_\theta^2 + \theta^2 \geq 1 \quad . \tag{45}$$

The critical thermal-maser transition line is then only dependent of the variance σ_θ^2 and the mean value θ:

$$a(\theta) = \frac{1}{2} + \frac{1}{2}\frac{1}{\sigma_\theta^2 + \theta^2} \quad . \tag{46}$$

For values of a and θ above this critical line, i.e. $a \geq a(\theta)$, the micromaser system is in a maser phase. Below this line, on the other hand, the micromaser is in the thermal phase (see e.g. Fig. 2).

The order parameter $\bar{x}(\theta)$ is continuous on the critical line Eq. (46). The first derivative of $\bar{x}(\theta)$ with respect to θ, $\bar{x}'(\theta)$, at this critical thermal-maser line is

$$\bar{x}'(\theta) = 6\,\frac{\theta}{\langle \xi^4 \rangle} \quad , \tag{47}$$

which is non-zero for $\sigma_\theta^2 < 1$. The critical line Eq. (46) then describes a line of second-order (thermal-maser) phase transition. If $\sigma_\theta^2 \geq 1$, Eq. (46) also describes a line of second-order phase transitions for all values of θ except for $\theta = 0$ where $a(0) = 1/2 + 1/(2\sigma_\theta^2)$. Since $\bar{x}'(\theta)$ then is zero we have to investigate higher order derivatives. The second derivative of $\bar{x}(\theta)$ with respect to θ, $\bar{x}''(\theta)$, at the critical thermal-maser line is

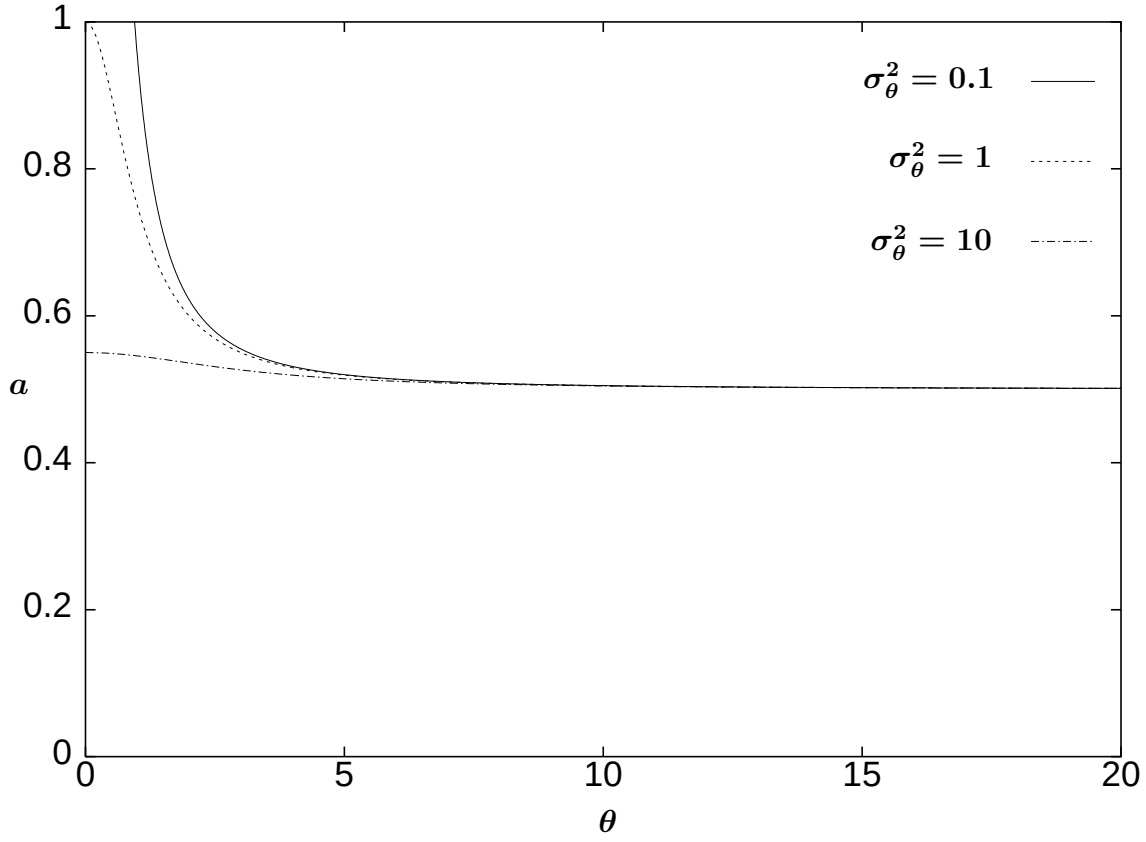

Figure 2: The thermal-maser critical lines $a(\theta)$ according to Eq. (46) for $\sigma_\theta^2 = 0.1, 1, 10$, i.e. when the micromaser is not detuned. All other parameters are as in Fig. 1. When $\sigma_\theta^2 \geq 1$ the critical thermal-maser line describes a third-order phase transition at $a(0) = 1/2 + 1/(2\sigma_\theta^2)$ and a second-order transition for any other possible value of a. When $\sigma_\theta^2 = 10$, this third-order phase transition occurs at $a(0) = 0.55$.

$$\bar{x}''(\theta) = \frac{6}{\langle \xi^4 \rangle} \left[1 - 2\frac{\theta}{\langle \xi^4 \rangle} \frac{d\langle \xi^4 \rangle}{d\theta} + \frac{7}{12} \left(\frac{\theta}{\langle \xi^4 \rangle} \right)^2 \langle \xi^6 \rangle \right] \quad , \tag{48}$$

which is non-zero when the first derivative $\bar{x}'(\theta)$ is zero. The point $a(0) = 1/2 + 1/(2\sigma_\theta^2)$ on the critical thermal-maser line therefore corresponds to a third-order transition. From Eq. (48) it follows, in addition, that we can have at most a third-order phase transition when fluctuations in θ are taken into account.

If the probability $P_\theta(\xi)$ is sufficiently peaked such that the its ξ-variation is fast in comparison to ξ-variation of $\sin^2(\xi\Delta)$, i.e. if $\sigma_\theta|\Delta| \ll \pi/2$, then Eq. (38) is reduced to $I_1(\theta) = \sin^2(\theta\Delta)/\Delta^2 + \sigma_\theta^2 \cos(2\theta\Delta)$. The first thermal-maser critical line is then given by

$$a(\theta) = \frac{1}{2} + \frac{1}{2}\frac{\Delta^2}{\sin^2(\theta\Delta) + \sigma_\theta^2\Delta^2\cos(2\theta\Delta)} \quad , \tag{49}$$

which is consistent with the result of Ref. [12] for $\sigma_\theta^2 = 0$.

If, on the other hand, the quantity $P_\theta(\xi)$ has a ξ-variation which is slow in comparison to the ξ-variation of $\sin^2(\xi\Delta)$ i.e. if $\sigma_\theta|\Delta| \gg \pi/2$, then Eq. (38) reduces to $I_1(\theta) = 1/2\Delta^2$. Eq. (41) is then reduced to

$$a(\theta) = \frac{1}{2} + \Delta^2 \quad . \tag{50}$$

In order to get explicit analytic results we now choose the following gamma probability distribution for the pump parameter

$$P_\theta(\xi) = \frac{\beta}{\Gamma(\alpha+1)}\,\xi^\alpha\, e^{-\beta\xi} \quad , \tag{51}$$

where $\beta = \theta/\sigma_\theta^2$ and $\alpha = \theta^2/\sigma_\theta^2 - 1$, so that $\langle\xi\rangle = \theta$ and $\langle(\xi-\theta)^2\rangle = \sigma_\theta^2$. Other choices are possible, but are not, as long as the distribution is sufficiently peaked, expected to change the overall qualitative picture. The integral $I_1(\theta, x)$ is then given by

$$\begin{aligned} I_1(\theta,x) &= \frac{1}{2}\,\frac{1}{x+\Delta^2} \\ &\times \left[\, 1 - \left(1 + \frac{2(x+\Delta^2)\sigma_\theta^2}{\theta^2/2\sigma_\theta^2}\right)^{-\frac{\theta^2}{2\sigma_\theta^2}} \cos\left(\frac{\theta^2}{\sigma_\theta^2}\arctan\left(\sqrt{\frac{2(x+\Delta^2)\sigma_\theta^2}{\theta^2/2\sigma_\theta^2}}\right)\right) \,\right]. \end{aligned} \tag{52}$$

This averaged form of $q(x)$ depends on the two independent variables $\theta^2/(2\sigma_\theta^2)$ and $2(x+\Delta^2)\,\sigma_\theta^2$ only. In particular, if

$$\frac{\theta^2}{2\sigma_\theta^2} \gg \sigma_\theta^2 \quad , \tag{53}$$

then Eq. (52) reduces to

$$I_1(\theta,x) = \frac{1}{2}\,\frac{1}{x+\Delta^2}\,\left[\, 1 - e^{-2(x+\Delta^2)\sigma_\theta^2}\,\cos\left(2\theta\sqrt{x+\Delta^2}\right) \,\right] \quad . \tag{54}$$

This explicit form of $I_1(\theta, x)$ can be achieved for a broad class of probability distributions, e.g. a Gaussian distribution. If, in addition,

$$\sigma_\theta^2 \gg \frac{1}{2a-1} \quad , \tag{55}$$

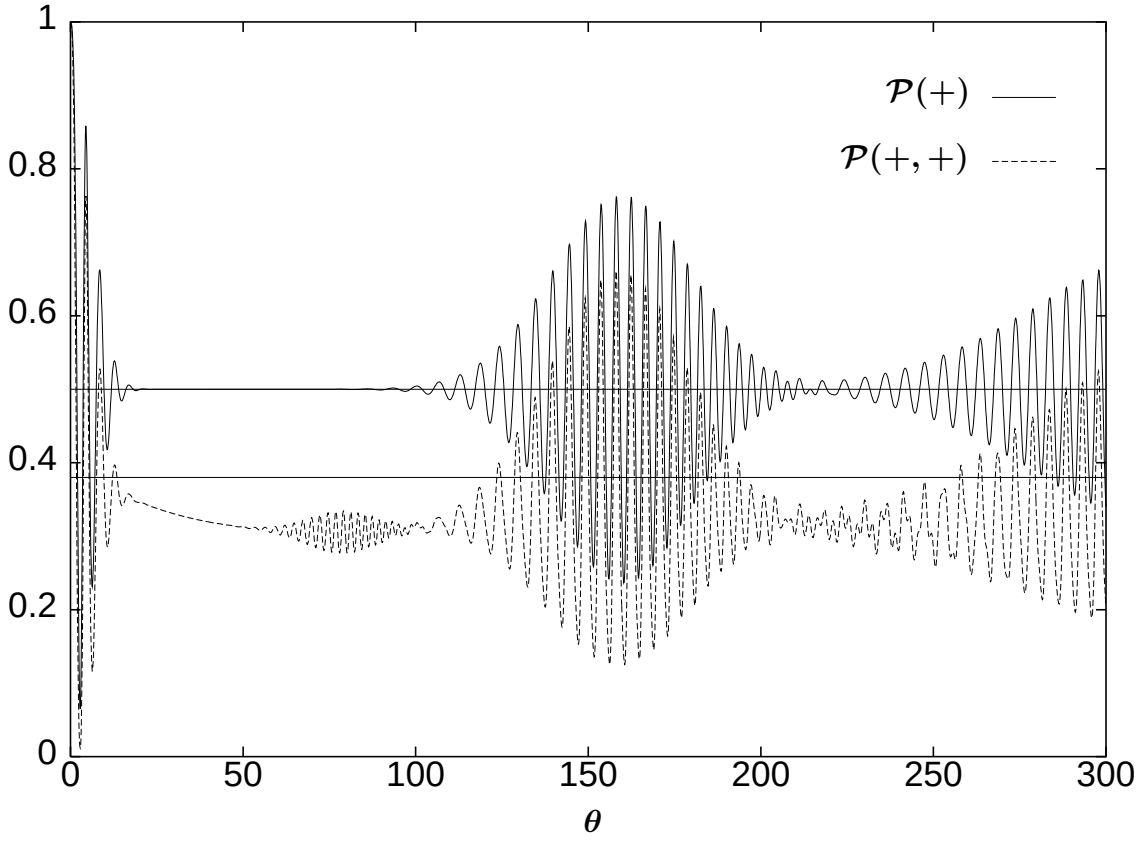

Figure 3: The probabilities $\mathcal{P}(+)$ (solid line) and $\mathcal{P}(+,+)$ (dotted line) as a function of θ when the q_m-terms in Eq. (2) are averaged with respect to θ with $\sigma_\theta^2 = 25$. All other parameters are as in Fig. 1. In the large θ limit the probability $\mathcal{P}(+)$ approaches $\mathcal{P}_\infty(+) = 0.5$ and the probability $\mathcal{P}(+,+)$ approaches $\mathcal{P}_\infty(+,+) \approx 0.38$, which are indicated by solid lines in the figure.

then any solution to the corresponding saddle-point equation $1 = (2a-1)I_1(\theta, x(\theta))$ is exponentially close to

$$\bar{x} = a - 1/2 - \Delta^2 \quad . \tag{56}$$

If, on the other hand,

$$\sigma_\theta^2 \gg \theta \gtrsim \sigma_\theta \gtrsim 1 \quad , \tag{57}$$

then the corresponding saddle-point equation has one non-trivial solution only, i.e. Eq. (56). Under the conditions given by Eqs. (53) and (55) or Eq. (57) the maser-maser phase transitions will be less significant. The phase diagram then essentially consists of critical thermal-maser line(s) only (see e.g. Fig. 2). With regard to the observable $\mathcal{P}(+)$, the requirement $\theta \gtrsim \theta_{\nu=1} = 2\pi N\sqrt{\bar{x} + \Delta^2}$ is compatible with Eq. (53) provided that N is sufficiently large, i.e.

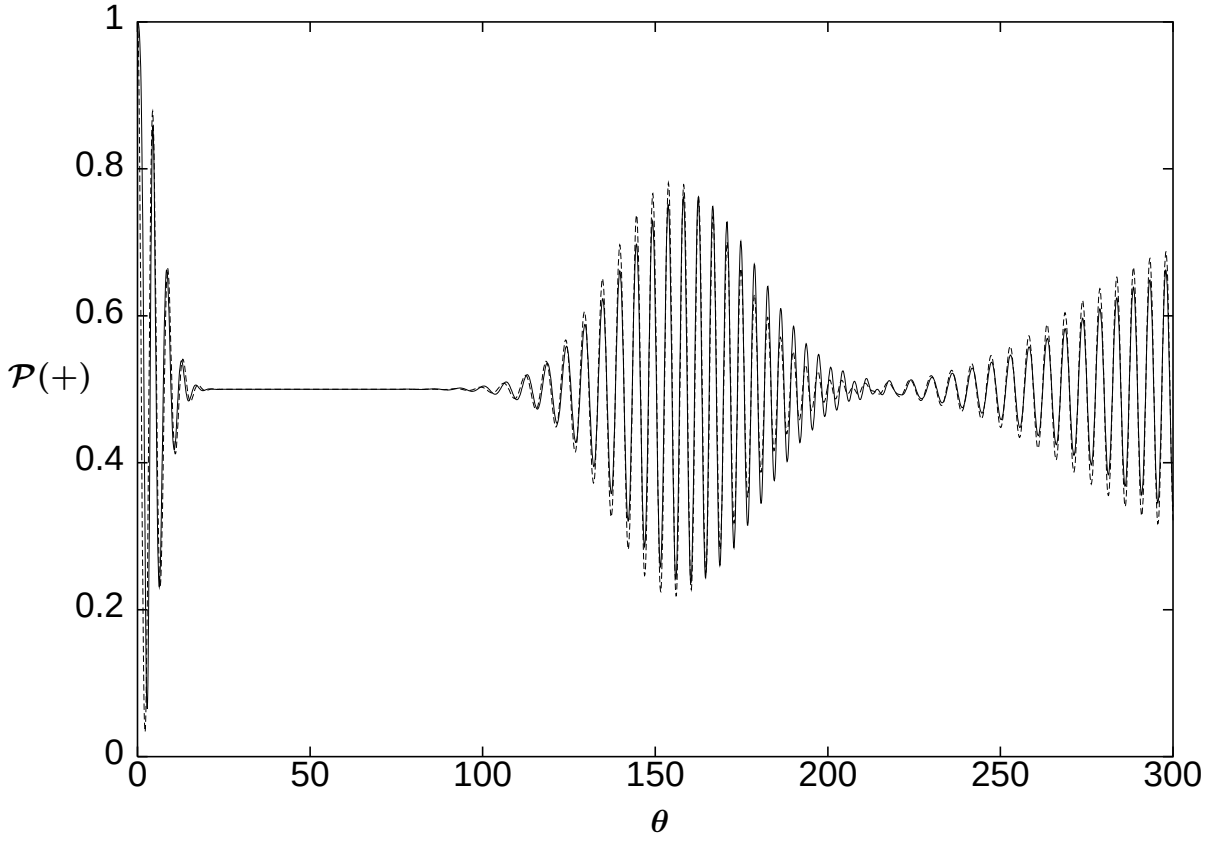

Figure 4: Comparison of the exact $\mathcal{P}(+)$ (solid line) and $\mathcal{P}(+)$ as given in Eq. (24) (dashed line) with $\bar{p}(x)$ as given in Eq. (18) with $\bar{x} = 1/2$. The parameters are the same as in Fig. 3. In this figure we only see the first two revivals, i.e. only the terms $\nu = 0, 1, 2$ in Eq. (24) is visible in this figure.

$$N \gg \frac{\sqrt{2}}{2\pi} \frac{\sigma_\theta^2}{\sqrt{a - 1/2}} \quad , \tag{58}$$

for the saddle-point solution Eq. (56). The equilibrium probability distribution is in this case given by Eq. (18) with the variance $\sigma_x^2 = [\, a + n_b(2a-1)\,]/2N$ and $x_j = \bar{x}$ as in Eq. (56). The equilibrium distribution $\bar{p}(x)$ is peaked around $\bar{x}$ provided $\bar{x} \gg \sigma_x$, i.e.

$$N \gg \frac{1}{2} \frac{a + n_b(2a-1)}{[\, a - 1/2 - \Delta^2\,]^2} \quad . \tag{59}$$

From Eq. (27) we observe that the ν:th revival in $\mathcal{P}(+)$ occurs in the region where θ is close to

$$\theta_\nu = 2\pi\nu N\sqrt{a - 1/2} \quad . \tag{60}$$

According to Eq. (29), two consecutive revivals in $\mathcal{P}(+)$ are separated provided

$$\nu < \sqrt{2N}\,\frac{2a-1}{\sqrt{a+n_b(2a-1)}} - \frac{1}{2} \quad , \tag{61}$$

which gives a bound on how many revivals that can be resolved in the excitation probability $\mathcal{P}(+)$. In Fig. 3 we consider values of relevant physical parameters such that Eqs. (55), (58) and (59) are satisfied. We then observe that $\mathcal{P}(+)$ and $\mathcal{P}(+,+)$ exhibit well pronounced revivals. For completeness we show in Fig. 4, for the same set of values of the physical parameters as in Fig. 3, that the approximative but analytical expression for $\mathcal{P}(+)$ as given by Eq. (24) is in very good agreement with the exact result for $\mathcal{P}(+)$. Within one standard deviation we expect, according to Eq. (61), that at most seven revivals in $\mathcal{P}(+)$ are well separated in this case. Numerically we find that actually only the first two revivals are well separated.

Let us now consider the case $\sigma_\theta^2 \ll 1$. If, in addition, Eq. (53) is satisfied, the quantity $\langle q(x)\rangle_\theta$ is reduced to Eq. (1). If on the other hand Eq. (53) is not satisfied, i.e. $\theta \ll \sigma_\theta^2$, then the saddle-point equation Eq. (20) has only the trivial solution for any probability distribution $P_\theta(\xi)$ as it should. The fluctuations in the atom cavity time have then no dramatic effect on the order parameter $\bar{x}$ (see e.g. Fig. 7), the excitation probabilities $\mathcal{P}(+)$ and $\mathcal{P}(+,+)$ or the phase diagram.

4.2 Detuning Fluctuations

In this Section we consider the situation when there is a spread in the detuning parameter Δ. Suppose that the spread in the detuning Δ is expressed in terms of a stochastic variable ξ as described by the probability distribution $P_\Delta(\xi)$ such that $\langle\xi\rangle = \Delta$ and $\langle(\xi-\Delta)^2\rangle = \sigma_\Delta^2$. The averaged value of $q(x)$ with respect to $P_\Delta(\xi)$ is then

$$\langle q(x)\rangle_\Delta = \int_{-\infty}^{\infty} d\xi\; P_\Delta(\xi)\,\frac{x}{x+\xi^2}\sin^2\left(\theta\sqrt{x+\xi^2}\right) \quad . \tag{62}$$

Non-trivial saddle-points of $V_0(x)$ can then be found by solving the equation

$$1 = (2a-1)\,J_1(\theta, x(\theta)) \quad , \tag{63}$$

where

$$J_1(\theta,x) = \theta^2 \int_{-\infty}^{\infty} d\xi\; P_\Delta(\xi)\,\frac{\sin^2(\,\theta\sqrt{x+\xi^2}\,)}{(\,\theta\sqrt{x+\xi^2}\,)^2} \leq \theta^2 \quad . \tag{64}$$

For small values of x we follow the argument of Section 4.1 concerning the critical thermal-maser phase transition line. The critical transition line is then

$$a(\theta) = \frac{1}{2} + \frac{1}{2}\frac{1}{J_1(\theta)} \leq 1 \quad , \tag{65}$$

where $J_1(\theta, 0) \equiv J_1(\theta)$. Eq. (65) coincides with the radius of convergence of the thermal probability distribution Eq. (11). In general we must use a combination of analytical and numerical methods, as in the case of $\sigma_\theta = 0$ [12], in order to get a detailed picture of the phase diagram.

If the probability $P_\Delta(\xi)$ is sufficiently peaked such that the its ξ-variation is fast in comparison to ξ-variation of $\sin^2(\theta\xi)$, i.e. if $\sigma_\Delta \theta \ll \pi/2$, then Eq. (64) is reduced to $J_1(\theta) = [\, 3\, \sin^2(\theta\Delta)/\Delta^2 + \theta^2\, \cos(2\theta\Delta) - 2\theta \sin(2\theta\Delta)/\Delta\,]/\Delta^2$. The first thermal-maser critical line is then given by

$$a(\theta) = \frac{1}{2} + \frac{1}{2}\frac{\Delta^2}{\sin^2(\theta\Delta) + \sigma_\Delta^2\, g(\theta)} \quad , \tag{66}$$

where $g(\theta) \equiv 3\, \sin^2(\theta\Delta)/\Delta^2 + \theta^2 \cos(2\theta\Delta) - 2\theta\, \sin(2\theta\Delta)/\Delta$, which is consistent with [12] for $\sigma_\Delta^2 = 0$.

If, on the other hand, the quantity $P_\Delta(\xi)$ has a ξ-variation which is slow in comparison to the ξ-variation of $\sin^2(\theta\xi)$, i.e. if $\sigma_\Delta \theta \gg \pi/2$, then $J_1(\theta)$ reduces to

$$J_1(\theta) = 1/2\Delta^2 \quad . \tag{67}$$

Eq. (66) is then reduced to

$$a(\theta) = \frac{1}{2} + \Delta^2 \quad . \tag{68}$$

In order to get explicit analytic results we now choose the following exponential probability distribution for the detuning parameter

$$P_\Delta(\xi) = \frac{1}{\sqrt{2\pi\sigma_\Delta^2}}\, \exp\left(-\frac{(\xi - \Delta)^2}{2\sigma_\Delta^2}\right) \quad , \tag{69}$$

such that $\langle \xi \rangle = \Delta$ and $\langle (\xi - \Delta)^2 \rangle = \sigma_\Delta^2$. Other choices are possible, but are not, as long as the distribution is sufficiently peaked, expected to change the overall qualitative picture. The averaged value of $q(x)$ with respect to $P_\Delta(\xi)$ is given by

$$\langle q(x) \rangle_\Delta = \langle q(x) \rangle_0 + \langle q(x) \rangle_{osc} \quad , \tag{70}$$

where

$$\langle q(x)\rangle_0 \equiv \frac{1}{2}\frac{x}{\sqrt{2\pi\sigma_\Delta^2}}\int_{-\infty}^{\infty} d\xi\ \frac{e^{-\frac{(\xi-\Delta)^2}{2\sigma_\Delta^2}}}{x+\xi^2} \quad , \tag{71}$$

and

$$\langle q(x)\rangle_{osc} \equiv -\frac{1}{2}\frac{x}{\sqrt{2\pi\sigma_\Delta^2}}\int_{-\infty}^{\infty} d\xi\ \frac{e^{-\frac{(\xi-\Delta)^2}{2\sigma_\Delta^2}}}{x+\xi^2}\ \cos\left(2\theta\sqrt{x+\xi^2}\right) \quad . \tag{72}$$

We observe that

$$\langle q(x)\rangle_0 = \sqrt{\frac{x}{2\sigma_\Delta^2}}\ e^{-\Delta^2/2\sigma_\Delta^2+x/2\sigma_\Delta^2}\int_{\sqrt{x/2\sigma_\Delta^2}}^{\infty} d\eta\ \exp\left[-\eta^2+\frac{1}{\eta^2}\frac{\Delta^2}{2\sigma_\Delta^2}\frac{x}{2\sigma_\Delta^2}\right] \quad . \tag{73}$$

Eq. (73) can be used to find an expansion in the parameter $\Delta^2/2\sigma_\Delta^2$. For our purposes we notice that if σ_Δ^2 is sufficiently large, i.e.

$$\sigma_\Delta^2 \gg 1 \quad , \tag{74}$$

then Eq. (73) is reduced to $\langle q(x)\rangle_0 \lesssim \frac{1}{2}\sqrt{\pi\, x/2\sigma_\Delta^2} + \mathcal{O}(\, x/2\sigma_\Delta^2\,)$. Any solution of the corresponding saddle-point equation is much less then unity since $\langle q(x)\rangle_{osc} \leq \langle q(x)\rangle_0$. The maser-maser phase transitions will therefore be less significant. The phase diagram does then essentially consist of critical thermal-maser line(s) only. For sufficiently large values of θ, i.e.

$$\theta \gg \frac{\sqrt{2\pi\sigma_\Delta^2}}{2a-1} \quad , \tag{75}$$

the oscillating term can be estimated by $|\langle q(x)\rangle_{osc}| \approx [\,\pi/8\sigma_\Delta^2\,]^{1/4}\,\sqrt{(2a-1)/(8\sigma_\Delta^2\theta)}$ for the solution

$$\bar{x} = (2a-1)^2\frac{\pi}{8\sigma_\Delta^2} \quad , \tag{76}$$

of the saddle-point equation. Eq. (76) is much less then unity due to the assumption Eq. (74). The term $\langle q(x)\rangle_{osc}$ is negligible in comparison to $\langle q(x)\rangle_0$ when Eq. (75) is satisfied. With regard to the observable $\mathcal{P}(+)$, the requirement $\theta \gtrsim \theta_{\nu=1} = 2\pi N\sqrt{\bar{x}+\Delta^2}$ is compatible with Eq. (75) provided that N is sufficiently large, i.e.

$$N \gg \frac{4}{\pi^3}\,\frac{2\sigma_\Delta^2}{(2a-1)^2} \quad , \tag{77}$$

for the solution Eq. (76) of the saddle-point equation. The equilibrium probability distribution is given by Eq. (18) with $x_j = \bar{x}$ as in Eq. (76) and $\sigma_x^2 = (2a-1)[\,a + n_b(2a-1)\,]\pi/(4N\sigma_\Delta^2)$. The probability distribution $\bar{p}(x)$ is therefore peaked around $\bar{x}$ provided that $\bar{x} \gg \sigma_x$, i.e.

$$N \gg \frac{16[\,a + n_b(2a-1)\,]}{(2a-1)^3\pi}\,\sigma_\Delta^2 \quad . \tag{78}$$

The ν:th revival of $\mathcal{P}(+)$ occurs in the region where θ is close to

$$\theta_\nu = (2a-1)\pi\sqrt{\frac{\pi}{2}}\frac{\nu N}{\sigma_\Delta} \quad , \tag{79}$$

according to Eq. (27). Eq. (29) implies that two consecutive revivals are separated provided that

$$\nu \leq \sqrt{\frac{N}{\sigma_\Delta^2}\,\frac{(2a-1)^3\pi}{16\,[a + n_b(2a-1)]}} - \frac{1}{2} \quad , \tag{80}$$

which gives a bound on how many revivals that can be resolved in the excitation probability $\mathcal{P}(+)$. Fluctuations in the atom cavity transit time with a large σ_θ^2 give, however, an order parameter of the order one. This difference between θ- and Δ-fluctuations is illustrated in Fig. 7. In Fig. 5 we consider physical parameters such that Eqs. (74), (77) and (78) are satisfied. We observe that $\mathcal{P}(+)$ and $\mathcal{P}(+,+)$ now exhibit well pronounced revivals. With the same set of physical parameters one can also verify that the approximative but analytical expression for $\mathcal{P}(+)$ as obtained by a Poisson resummation technique, i.e. Eq. (24), is in good agreement with the exact expression for $\mathcal{P}(+)$. We also notice that according to Eq. (80), only the first revival in $\mathcal{P}(+)$ is clearly resolved in this case, which agrees well with our numerical results.

Let us now, on the other hand, consider the case when σ_Δ^2 is small but non-zero, i.e.

$$0 < \sigma_\Delta^2 \ll 1 \quad . \tag{81}$$

The quantity $\langle q(x)\rangle_0$ can then be approximated according to $\langle q(x)\rangle_0 = x/[\,2(x+\Delta^2)\,]$ and the term $\langle q(x)\rangle_{osc}$ has an upper bound $|\langle q(x)\rangle_{osc}| \leq 1/[\,1+\epsilon^2\,]^{1/4}$, where $\epsilon \equiv 2\sigma_\Delta^2\theta x/(\,x + \Delta^2\,)^{3/2}$. For sufficiently large values of θ, i.e.

$$\theta \gg \frac{1}{2\sigma_\Delta^2}\,\frac{(a-1/2)^{3/2}}{a-1/2-\Delta^2} \quad , \tag{82}$$

the term $\langle q(x)\rangle_{osc}$ is negligible in comparison to $\langle q(x)\rangle_0$ for the solution

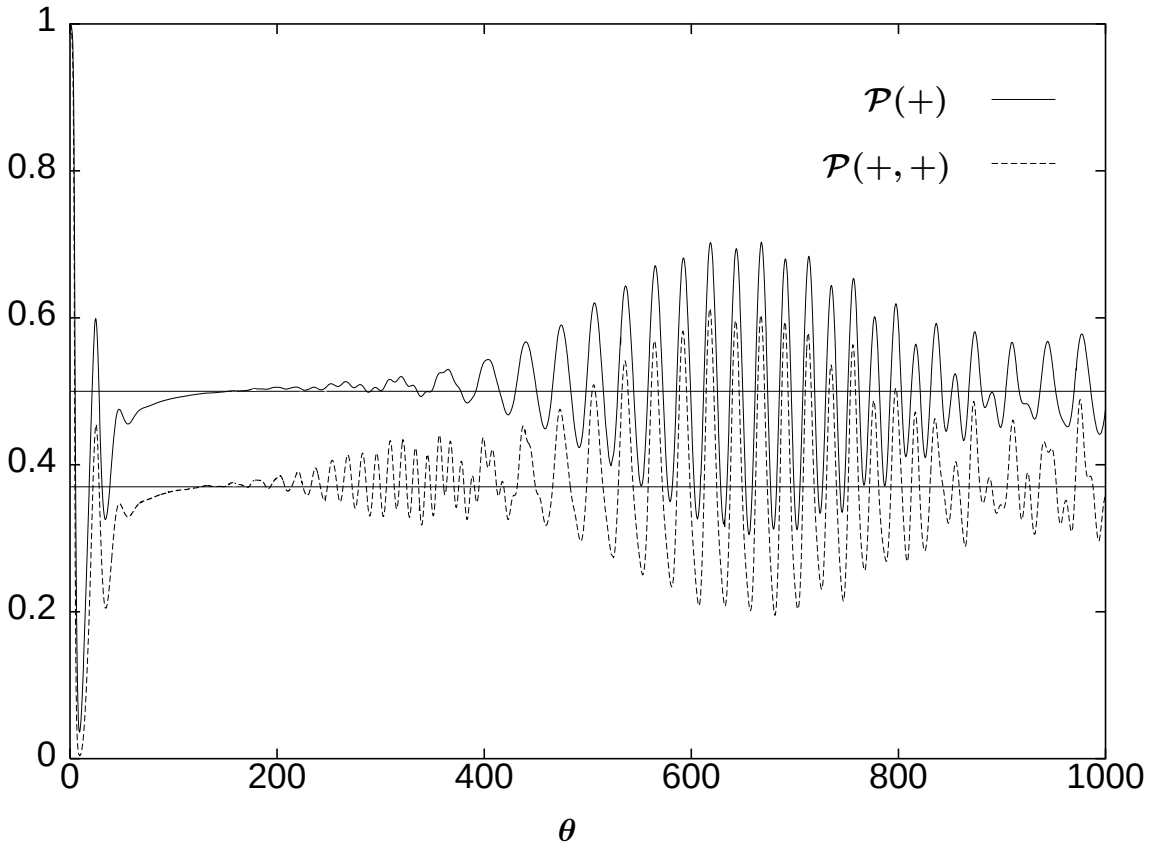

Figure 5: The probabilities $\mathcal{P}(+)$ (solid line) and $\mathcal{P}(+,+)$ (dotted line) as a function of θ when the q_m-terms in Eq. (2) are averaged with respect to Δ with $\sigma_\Delta^2 = 25$ and $N = 800$. All other parameters are as in Fig. 1. In the large θ and N limit the probability $\mathcal{P}(+)$ approaches $\mathcal{P}_\infty(+) = 0.5$ and the probability $\mathcal{P}(+,+)$ approaches $\mathcal{P}_\infty(+,+) \approx 0.38$, as indicated by a solid line in the figure. For sufficiently large θ, $\bar{x} \approx 0.02$ and $\langle \mathcal{P}(+) \rangle \approx \langle \mathcal{P}(+,+) \rangle \approx 1$.

$$\bar{x} = a - 1/2 - \Delta^2 \quad , \tag{83}$$

of the saddle-point equation. The maser-maser phase transitions will therefore be less significant if Eqs. (81) and (82) are satisfied. The phase diagram does then essentially consist of critical thermal-maser line(s) only. For sufficiently small values of θ, i.e.

$$\theta \ll \frac{1}{2\sigma_\Delta} \quad , \tag{84}$$

Eq. (70) is reduced to Eq. (1). Hence there is no dramatic change in the order parameter or in the phase diagram. With regard to the observable $\mathcal{P}(+)$, the requirement $\theta \gtrsim \theta_{\nu=1} = 2\pi N\sqrt{\bar{x} + \Delta^2}$ is compatible with Eq. (82) provided that N is sufficiently large, i.e.

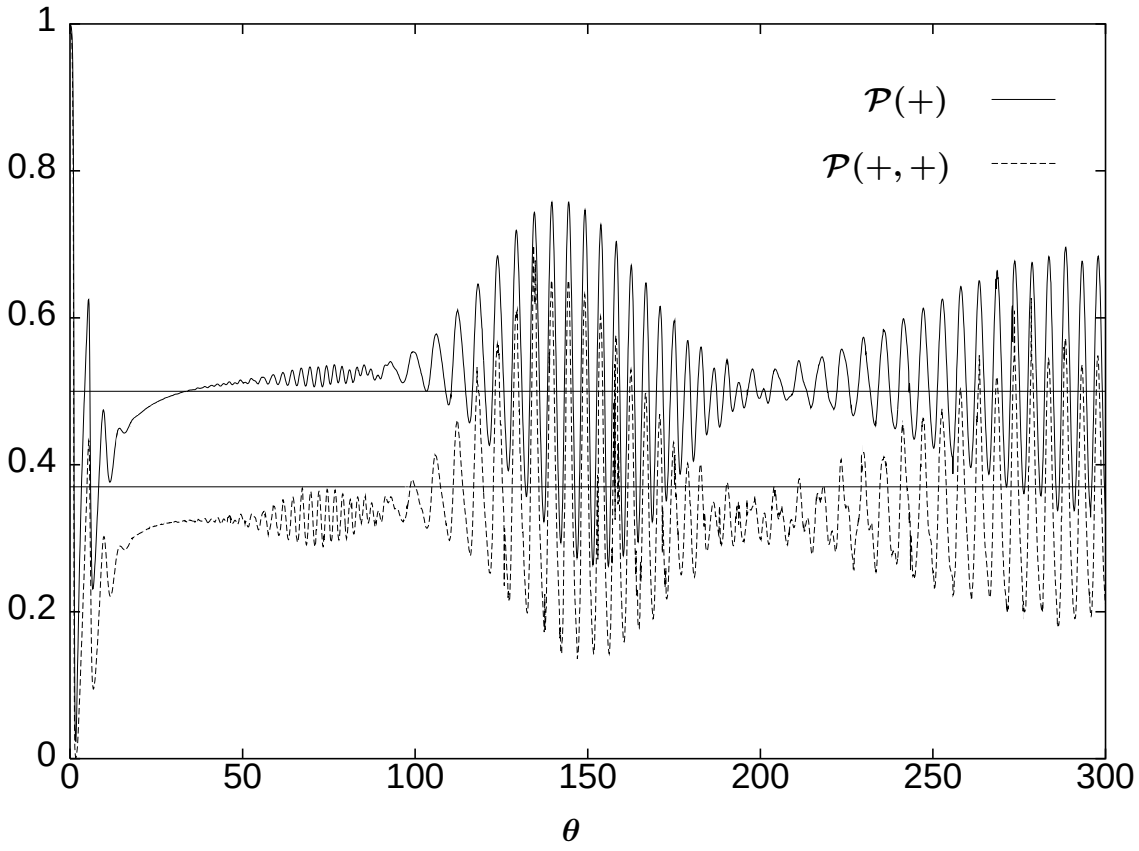

Figure 6: The probabilities $\mathcal{P}(+)$ (solid line) and $\mathcal{P}(+,+)$ (dotted line) as a function of θ when the q_m-terms in Eq. (2) are averaged with respect to Δ with $\sigma_\Delta^2 = 0.1$ All other parameters are as in Fig. 1. In the large θ and N limit the probability $\mathcal{P}(+)$ approaches $\mathcal{P}_\infty(+) = 0.5$ and the probability $\mathcal{P}(+,+)$ approaches $\mathcal{P}_\infty(+,+) \approx 0.38$, which is indicated by a solid line in the figure. For sufficiently large θ, $\bar{x} \approx 0.5$, $\langle \mathcal{P}(+) \rangle \approx 0.5$ and $\langle \mathcal{P}(+,+) \rangle \approx 0.38$.

$$N \gg \frac{1}{4\pi\sigma_\Delta^2} \, \frac{\sqrt{a-1/2}}{a-1/2-\Delta^2} \quad . \tag{85}$$

The equilibrium probability distribution is then given by Eq. (18) with $x_j = \bar{x}$ as in Eq. (83) and $\sigma_x^2 = [\, a + n_b(2a-1)\,]/(2N)$ according to Eq. (19). The distribution $\bar{p}(x)$ is peaked around $\bar{x}$ provided that $\bar{x} \gg \sigma_x$, i.e.

$$N \gg \frac{1}{2} \, \frac{a + n_b(2a-1)}{a-1/2-\Delta^2} \quad . \tag{86}$$

The ν:th revival of $\mathcal{P}(+)$ occurs in the region where θ is close to

$$\theta_\nu = 2\pi\nu N \sqrt{a-1/2} \quad , \tag{87}$$

according to Eq. (27). Furthermore, two consecutive revivals are separated provided that

$$\nu \leq \sqrt{\frac{N}{2}\,\frac{(2a-1)^2}{a+n_b(2a-1)}} - \frac{1}{2} \quad , \tag{88}$$

which gives a bound on how many revivals that can be resolved in the excitation probability $\mathcal{P}(+)$.

In Fig. 6 we consider physical parameters such that Eqs. (81), (85) and (86) are satisfied. In this case we also observe well pronounced revivals in $\mathcal{P}(+)$ and $\mathcal{P}(+,+)$. The width and location of the revival in $\mathcal{P}(+)$ agrees well with the approximative expression Eq. (24).

5 The Correlation Length

Let us now consider long-time correlations in the large N limit as was first introduced in Ref.[9]. These correlations are most conveniently obtained by making use of the continuous time formulation of the micromaser system [10]. The lowest eigenvalue $\lambda_0 = 0$ of the matrix L, as defined in Section 2, then determines the stationary equilibrium solution vector $p = \bar{p}$ as given by Eq. (2). The next non-zero eigenvalue λ of L, which we determine numerically, will then determine typical scales for the approach to the stationary situation. The joint probability for observing two atoms, with a time-delay t between them, can now be used in order to define a correlation length $\gamma^A(t)$ [9]. At large times $t \to \infty$, we define the atomic beam correlation length ξ_A by [9]

$$\gamma_A(t) \simeq e^{-t/\xi_A} \quad , \tag{89}$$

which then is determined by λ, i.e. $\gamma\xi_A = 1/\lambda$. For photons, we define a similar correlation length ξ_C. It follows that the correlation lengths are identical, i.e. $\xi_A = \xi_C \equiv \xi$ [9].

The correlation length $\gamma\xi$ is shown in Fig. 8 for different values of σ_θ^2 and exhibits large peaks for the pump parameters θ^*_{kk+1}, θ^*_0 and/or θ^*_{tk} [12]. The correlation grows at most as $\sqrt{N}$ at $\theta = \theta^*_0$. At θ^*_{kk+1} and θ^*_{tk} the large N dependence is, however, different. At these values of the pump parameter there is instead a competition between two neighbouring minima of $V_0(x)$. Using the technique of [9] it can be shown that the peak close to $\theta = \theta^*_{kk+1}$ is

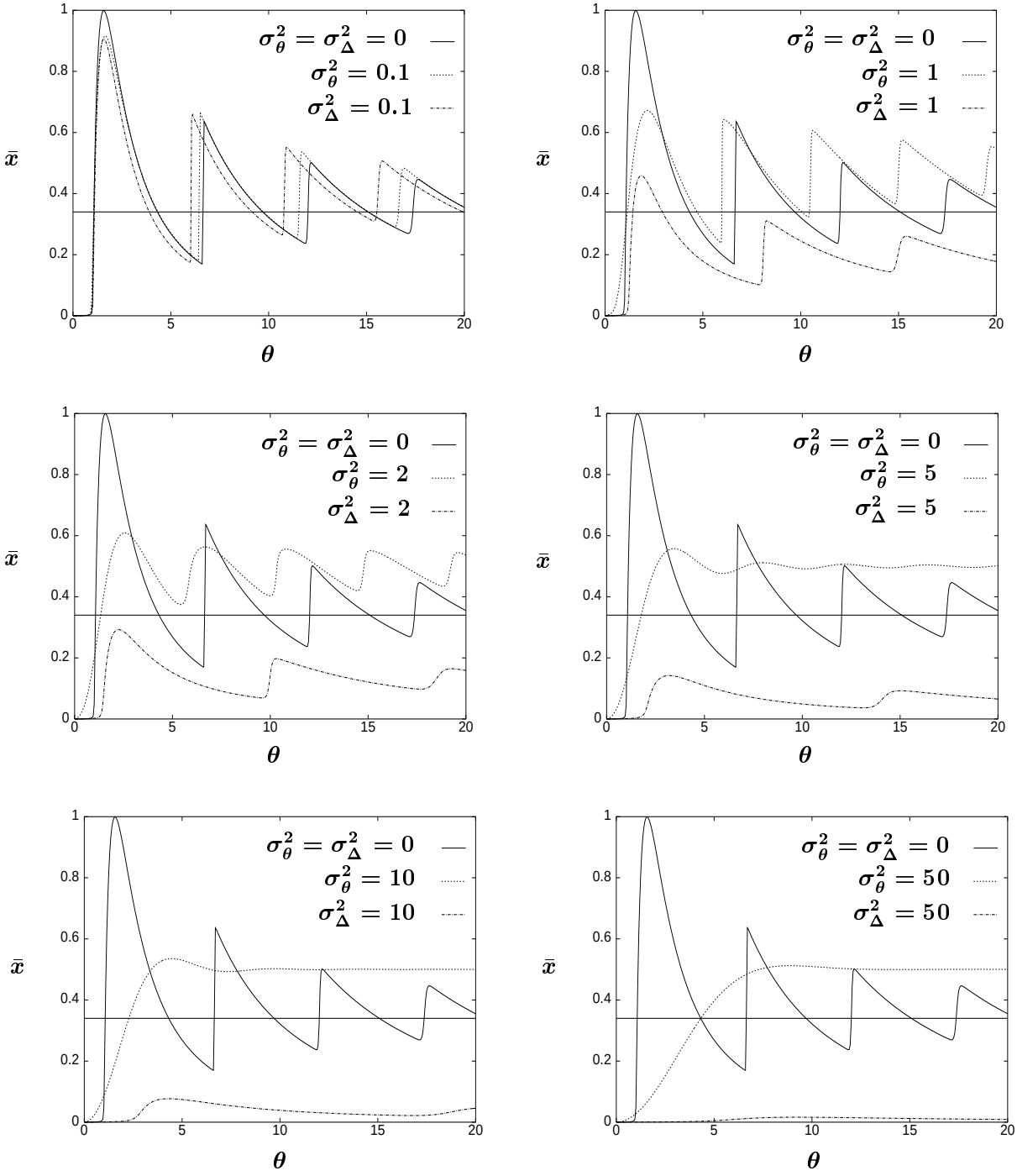

Figure 7: The normalized steady-state mean photon number $\bar{x} = \bar{n}/N$ as a function of θ for different values of σ_θ^2 and σ_Δ^2 when $a = 1$, $n_b = 0.15$, $\Delta = 0$ and $N = 1000$. In the large θ and N limit the order parameter approaches a constant value. This asymptotic value is determined by Eq. (33) when $\sigma_\theta^2 = \sigma_\Delta^2 = 0$. The solid line at $\bar{x}_\infty \approx 0.34$ in the figure corresponds to this asymptotic value of the order parameter.

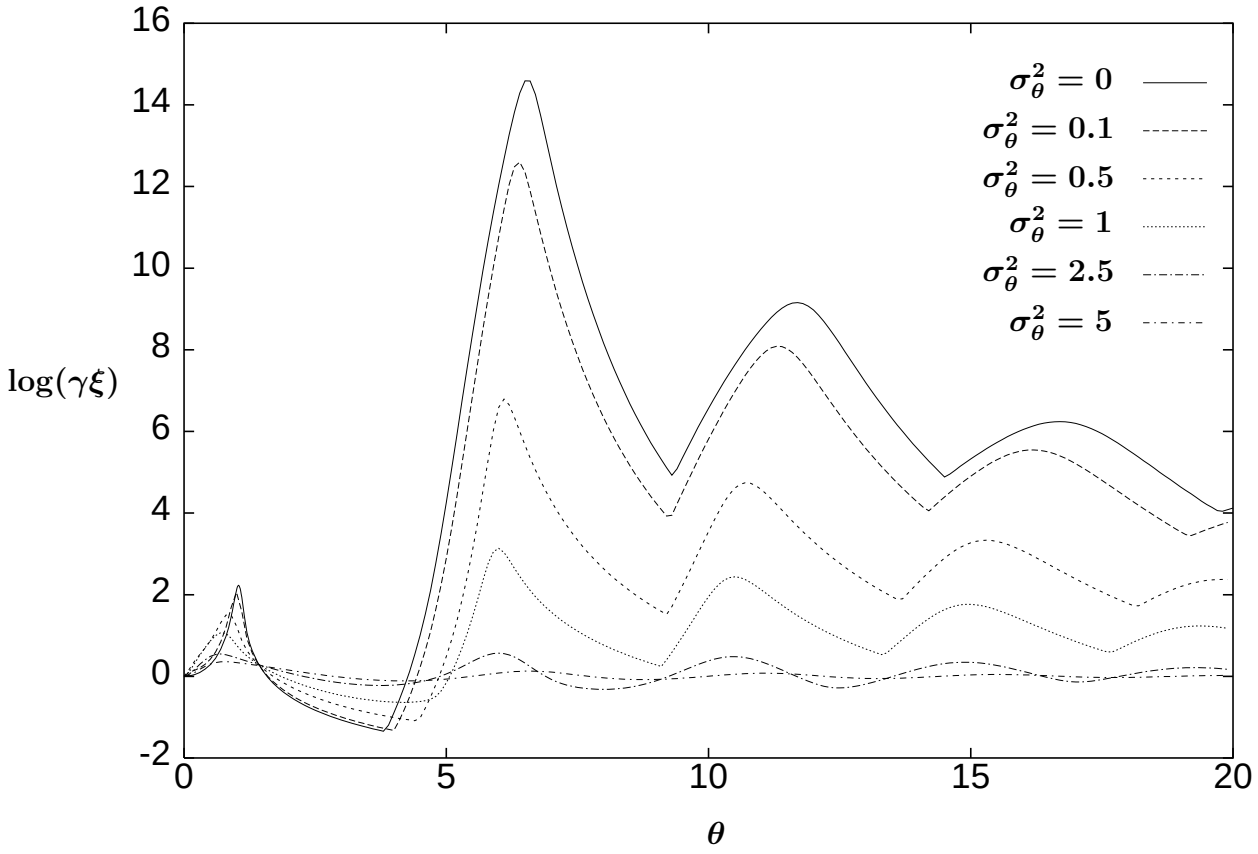

Figure 8: The logarithm of the correlation length $\gamma\xi$ as a function of θ for various values of $\sigma_\theta^2 = 0, 0.1, 0.5, 1, 2.5$ and 5 when $N = 100$, $n_b = 0.15$, $\Delta = 0$ and $a = 1$.

$$\gamma\xi \simeq e^{N\Delta V_0} \quad , \tag{90}$$

where ΔV_0 is the smallest potential barrier between the two competing minima of the effective potential $V_0(x)$. For increasing values of σ_θ^2 or σ_Δ^2 this potential barrier ΔV_0 decreases. The corresponding correlation length will then also decrease (see e.g. Fig. 8). Numerical study shows that adding fluctuations to the atom-photon frequency detuning result in the same quantitative effect: the peaks in the correlation length decreases due to smaller potential barriers ΔV_0.

6 Conclusion

In conclusion, we have investigated various effects of including noise-producing mechanisms in a micromaser system, like a velocity spread in the atomic beam or a spread in the atom-photon frequency detuning. For sufficiently large widths of the corresponding probability distributions, i.e. for sufficiently large σ_θ^2 or a non-zero σ_Δ^2, the excitation probabilities of atoms leaving the microcavity exhibit well-pronounced revivals. Noise therefore tends to increase the order in the system. Furthermore, the maser-maser phase transition disappear for sufficiently large σ_θ^2 or σ_Δ^2, in which case the phase diagram in the a- and θ- parameter space consists essentially of a single maser-thermal critical line. We have also shown that the correlation length drastically decreases when noise-producing mechanisms are included in the system.

APPENDIX

In this Appendix we derive an exact analytical expression for $V_0(x)$ in the large θ limit when the quantity q_n has no spread in any of the physical parameters, i.e. when $q(x)$ is as given in Eq. (1). The potential $V_0(x)$ may then be re-written in the from

$$\begin{aligned} V_0(x) &= -\int_0^x d\nu \Big\{ \ln\left[a\frac{\nu}{\nu+\Delta^2}+n_b\nu\right] + \ln\left[1+\frac{a\sin^2(\theta\sqrt{\nu+\Delta^2})-a}{a+n_b(\nu+\Delta^2)}\right] \\ &- \ln\left[b\frac{\nu}{\nu+\Delta^2}+(1+n_b)\nu\right] - \ln\left[1+\frac{b\,\sin^2(\theta\sqrt{\nu+\Delta^2})-b}{b+(1+n_b)(\nu+\Delta^2)}\right]\Big\} \quad . \end{aligned} \tag{91}$$

By making use of the power series expansion of the logarithm we obtain

$$\begin{aligned} V_0(x) &= -\int_0^x d\nu \Big\{ \ln\left[\left(b\,\frac{\nu}{\nu+\Delta^2}+(1+n_b)\nu\right) / \left(a\,\frac{\nu}{\nu+\Delta^2}+n_b\nu\right)\right] \\ &+ \sum_{n=1}^{\infty}\frac{1}{n}\Big[\left(\frac{a}{a+n_b(\nu+\Delta^2)}\right)^n - \left(\frac{b}{b+(1+n_b)(\nu+\Delta^2)}\right)^n\Big]\cos^{2n}(\theta\sqrt{\nu+\Delta^2})\Big\} \quad . \end{aligned} \tag{92}$$

In the large θ limit only the non-oscillating terms in Eq. (92) contribute, i.e.

$$V_0(x) = \int_0^x d\nu \left\{ \ln\left[\frac{1-a}{a}\right] + f(\,y(\nu)\,) - f(\,w(\nu)\,)\right\} \quad , \tag{93}$$

where

$$f(z) = \ln z + R(z) \quad , \tag{94}$$

and $y(x) = a/(\,a+n_b(x+\Delta^2)\,)$ and $w(x) = b/(\,b+(1+n_b)(x+\Delta^2)\,)$. The function $R(z)$ is defined by

$$R(z) = \sum_{n=1}^{\infty}\frac{1}{n}\frac{1}{2^{2n}}\frac{(2n)!}{(n!)^2}\,z^n \quad , \tag{95}$$

which is a generalized hypergeometric series [14]. By differentiating Eq. (93) we therefore, finally, obtain Eq. (33).

ACKNOWLEDGEMENT

The authors wish to thank the members of NORDITA for the warm hospitality while the present work was completed. The research has been supported in part by the Research Council of Norway under contract no. 118948/410.

References

[1] Y. Yamamoto and H.A. Haus "*Preparation, Measurement and Information Capacity of Optical Quantum States*", Rev. Mod. Phys. **58** (1986) 1001; Y.I. Vorontsov "*Standard Quantum Limits of Measurement Errors and Methods of Overcoming Them*", Sov. Phys. Usp. **37** (1994) 81; C.M. Caves and P.D. Drummond "*Quantum Limits on Bosonic Communication Rates*", Rev. Mod. Phys. **66** (1994) 482; C.H. Henry and R.F. Kazarinov "*Quantum Noise in Photonics*", Rev. Mod. Phys. **68** (1996) 801.

[2] A. Maritan and J.R. Banavar, "*Chaos, Noise and Synchronization*", Phys. Rev. Lett. **72** (1994) 1451; L. Gammaitoni, P. Hänggi, P. Jung and F. Marchesoni "*Stochastic Resonance*", Rev. Mod. Phys. **70** (1998) 223; J.W.C. Robinson, D.E. Asraf, A.R. Bulsara and M.E. Inchiosa, "*Information-Theoretic Distance Measures and a Generalization of Stochastic Resonance*", Phys. Rev. Lett. **81** (1998) 2850; H. Zhonghuai, Y. Lingfa, X. Zuo and X. Houwen, "*Noise Induced Pattern Transition and Spatiotemporal Stochastic Resonance*", Phys. Rev. Lett. **81** (1998) 2854; G. Giacomelli, F. Marin and I. Rabbiosi, "*Stochastic and Bona Fide Resonance: An Experimental Investigation*", Phys. Rev. Lett. **82** (1999) 675; S. Kim, S. Hee Park and H.-B. Pyo, "*Stochastic Resonace in Coupled OScillator Systems with Time Delay*", Phys. Rev. Lett. **82** (1999) 1620; D. Nozaki, D.J. Mar, P. Grigg and J.J. Collins, "*Effects of Colored Noise on Stochastic Resonance in Sensory Neurons*", Phys. Rev. Lett. **82** (1999) 2402; T. Ohira and Y. Sato, "*Resonace with Noise and Delay*", Phys. Rev. Lett. **82** (1999) 2811; V.S. Anishchenko, A.B. Neiman, F. Moss and L. Schimansky-Geier "*Stochastic Resonace: Noise-Enhanced Order*", Sov. Phys. Usp. **42** (1999) 7; Y. L. Klimontovich "*What are Stochastic Filtering and Stochastic Resonance?*", Sov. Phys. Usp. **42** (1999) 37.

[3] A. Buchleitner and R.N. Mantegna, "*Quantum Stochastic Resonance in a Micromaser*", Phys. Rev. Lett. **80** (1998) 3932.

[4] H. Walther, "*The Single Atom Maser and the Quantum Electrodynamics in a Cavity*", Physica Scripta **T23** (1988) 165; "*Experiments on Cavity Quantum Electrodynamics*", Phys. Rep. **219** (1992) 263; "*Experiments With Single Atoms in Cavities and Traps*" in "*Fundamental Problems in Quantum Theory*", Eds. D.M. Greenberger and A. Zeilinger, Ann. N.Y. Acad. Sci. **755** (1995) 133; "*Single Atom Experiments in Cavities and Traps*", Proc. Roy. Soc. **A454** (1998) 431; "*Quantum Optics of a Single Atom*", Laser Physics **8** (1998) 1 and in Physica Scripta **T76** (1998) 138.

[5] B. W. S. and P. L. Knight, "*The Jaynes-Cummings Model*", J. of Mod. Opt. **40** (1993) 1195.

[6] "Nonclassical Effects in Quantum Optics", Eds. P. Meystre and D.F. Walls (AIP, 1991).

[7] B.-S. Skagerstam in "*Applied Field Theory* ", Eds. Choonkye Lee, Hyunsoo Min and Q-Han Park (Chungbum Publ. Hose, Seoul, 1999).

[8] D. Filipowicz, J. Javanainen and P. Meystre, "*The Microscopic Maser*", Opt. Comm. **58** (1986) 327; "*Theory of a Microscopic Maser*" Phys. Rev. **A34** (1986) 3077.

[9] P. Elmfors, B. Lautrup and B.-S. Skagerstam, "*Correlations as a Handle on the Quantum State of the Micromaser*", CERN/TH 95-154 (cond-mat/9506058); Physica Scripta **55** (1997) 724; "*Correlations in the Micromaser*" Phys. Rev. **A54** (1996) 5171.

[10] L. Lugiato, M. Scully and H. Walther, "*Connection Between Microscopic and Macroscopic Maser Theory*", Phys. Rev. **A36** (1987) 740.

[11] E.T. Jaynes and F.W. Cummings, "*Comparison of Quantum and Semiclassical Radiation Theories With Application of the Beam Maser*", Proc. IEEE **51** (1963) 89.

[12] P.K. Rekdal and B.-S. Skagerstam, "*On the Phase Structure of the Micromaser System*", Opt. Commun. 184 (2000) 195 and "*Theory of the Microscopic Maser Phase Transitions*", CERN-TH/99-410 (submitted for publication).

[13] M. Fleischhauser and W.P. Schleich, "*Revivals made simple: Poisson summation formula as a key to the revivals in the Jaynes-Cummings model*", Phys. Rev. **A47** (1993) 4258; R. Courant and D. Hilbert, "*Methods of Mathematical Physics*", Intersience, New York, 1953.

[14] A. Erdélyi, W. Magnus, F. Oberhetter and F. G. Tricomi, "*Higher Transcendental Functions*", McGraw-Hill Book Company, Volume I, 1953.